047

048

065

067

072

074

079

080

082

083

086

091

Subsurface Insight: Spatio-Temporal Embeddings for Hydrogeological Time Series Analysis

Abstract

002

003

004

005

006

007

008

010

011

012

013

014

015

018

019

020

021

022

023

025

026

027

028

029

031

032

0.33

034

035

036

037

039

040

041

042

043

044

045

The generation of terabytes of hydrogeological sensor data each year has driven a growing demand for hydrological data analysis to aid in water resource prediction and management. However, these data present complex spatio-temporal dependencies, especially for large-scale data. Traditional statistical methods like PCA often fail to capture nonlinear temporal patterns, and existing deep learning approaches do not effectively focus on integrating spatial context. This paper introduces a deep spatio-temporal autoencoder architecture to learn embeddings from decades of French groundwater level data. By using contrastive learning, we combine time series and their geographical coordinates to generate low-dimensional embeddings. We demonstrate that these embedding vectors are highly effective for downstream tasks, unsupervised clustering, compared with traditional methods. Crucially, our approach achieves a Normalized Mutual Information (NMI) score exceeding 0.55 against an expert-labeled ground truth, confirming that the learned representations capture physically meaningful subsurface characteristics.

Introduction 1

Understanding groundwater level is essential for managing groundwater resources, supporting forecasting and assessing geological hazards. Nowadays, modern sensors generate vast amounts of continuous data, but extracting meaningful patterns is always challenging due to noise, non-linearities, and intricate dependencies across multiple temporal and spatial scales. While traditional statistical methods like PCA are limited by their linearity and inability to handle sequential data, or models like ARIMA do not work well for Long-term time series data. To address these limitations, we propose a deep learning framework for spatio-temporal representations from hydrogeological data. With the contributions: (1) We introduce a autoencoder architecture using CNN and MLP-Mixers [1] for long-range dependency, (2) We demonstrate that adding spatial coordinates significantly improves the quality of embedding vectors (3) we also demonstrate that the embedding vectors from our model capture a classification structure that strongly aligns with expert-defined labels.

2 Methodology

Data and Preprocessing 2.1

We use a large-scale dataset from France since 1960 [2]. Let the initial raw dataset be denoted as $\mathcal{D}_{\text{raw}} = \{(X_i, C_i)\}_{i=1}^N$, where X_i is the raw time series from sensor i, and C_i represents its geographical coordinates. First, missing values are filled using surrounding values. However, to avoid affecting the distribution of the data when sampling, any time series with a continuous gap exceeding 30 days is segmented at the missing. This process each original series X_i into a set of one or more continuous sub-series, or segments, $\{S_{i,1}, S_{i,2}, ..., S_{i,k_i}\}$, where $k_i \geq 1$. Next, each outlier in segment $S_{i,j}$ is removed using the interquartile range (IQR) method, where any data point outside the range is clipped. 062 After that, we apply two-step normalization. First, a Box-Cox power transformation is applied to stabilize variance. Then, we apply Z-score normalization to ensure consistency across the entire data set.

Finally, our dataset is a collection of all normalized segments, each paired with its original sensor's normalized coordinates, denoted as $\{(S'_{i,j}, C'_i)\}$. This structure is specifically designed for our contrastive learning framework, where any two segments originating from the same sensor i (e.g., $S'_{i,j}$ and $S'_{i,l}$) constitute a positive pair.

2.2Model Architecture.

Our model is an autoencoder inspired by TimeMixer [3, 4] and uses a convolutional neural network (CNN) [5]. As illustrated in the figure 1, it processes two inputs: a time series window $W \in \mathbb{R}^{L \times 1}$ and its geographical coordinates $C \in \mathbb{R}^2$.

The core of the **encoder** consists of two parallel processing paths followed by a fusion layer. The time series path first processes the input window Wthrough a series of 1D CNN blocks (A) to extract a hierarchy of local features. These features are then combined by several Mixer Blocks to capture longrange connections. Concurrently, the spatial path processes the geographical coordinates C by an MLP to produce a location embedding. Crucially, the outputs from both the temporal path and the spatial path are then **concatenated** and passed through a final fusion layer (MLP) to create the latent embedding e. The latent embedding e serves as the

094

095

096

097

098

099

102

103

104

105

106

107

108

109

110

112

113

117

119

120

121

134

143

150

151

input for two downstream heads, each corresponding to a distinct training objective. First, it is passed to the **decoder**, which reconstructs the original time series \hat{W} using a U-Net-like architecture to ensure high-fidelity output [6]. Second, e is fed through a **projection head** for the contrastive learning task.

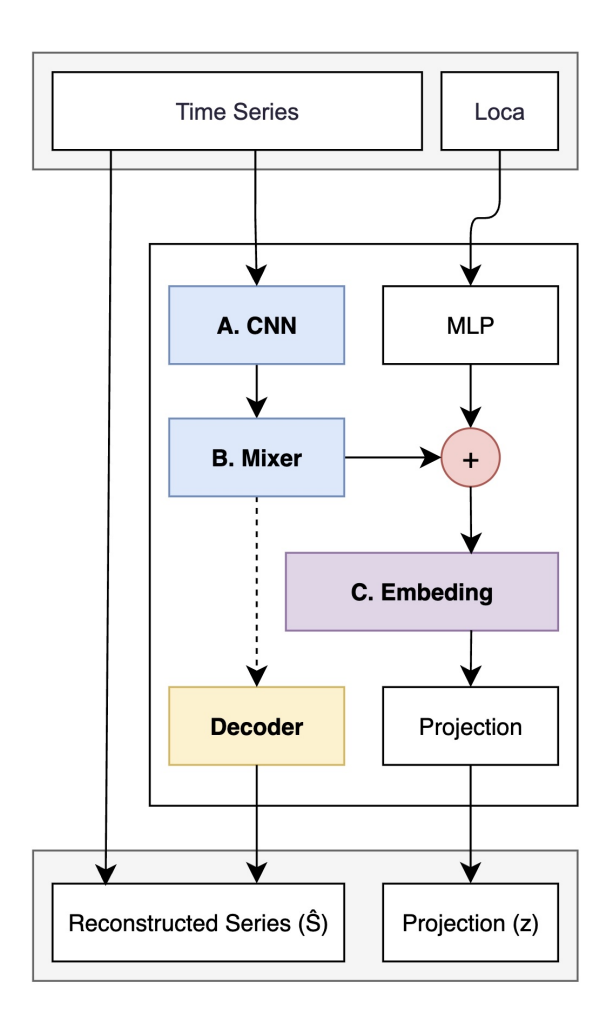


Figure 1. Our final architecture, henceforth referred to as 'Our Model', consists of a CNN branch for local feature extraction and an MLP-Mixer branch for long-range dependencies

Training Objective, the model is trained endto-end to minimize a composite loss function, which combines a reconstruction objective and a contrastive learning objective:

$$\mathcal{L}_{total} = \mathcal{L}_{contrastive} + \alpha \mathcal{L}_{recon}$$

Here, $\mathcal{L}_{\text{recon}}$ is the Mean Squared Error (MSE) between W and \hat{W} and The hyperparameter α is a weighting factor that balances the contribution of the reconstruction loss. For the contrastive task, we pass the embedding e through a projection and compute the NT-Xent loss [7], which encourages similar time series to have closer embeddings in the projection space. After training, only the encoder and fusion modules are used for downstream tasks.

3 Results and Analysis

We trained our model on a training set of 8,805 segments, validating on 2,202 segments. Models were trained using the Adam optimizer with a learning rate of 10^{-4} and early stopping. The evaluation of the embedding quality was done in two stages.

First, to validate our architectural design choices, we conducted an ablation study comparing our full model against several variants using internal clustering metrics (k=4). Our full proposed architecture is denoted as "Our Model". We compare it against a PCA baseline and key architectural variants to justify our design choices. The results are summarized in Table 1. Our full model achieves the highest Silhouette Score and lowest WCSS. Notably, (Our Model (no loca)) significantly decreases performance, confirming the importance of integrating spatial information.

Second, to validate embedding vectors quality in the real-world, we use a small dataset, experts classified it into "IG" sectors based on geological, hydrogeological, topographical, and administrative criteria, which were used as reference labels in the BSN study [8] to evaluate clustering performance, we clustered the embedding vectors into **66 groups**, corresponding to the number of labeled. This comparison yielded a **Normalized Mutual Information (NMI) score exceeding 0.55**, which shows a strong correspondence of our clustering with the expert classification, and indicates that the model has learned to capture hydrologically significant features.

Table 1. Comparison of clustering performance. "Our Model (CNN+Mixer)" is our full proposed architecture. Bold values indicate the best result for each metric. For WCSS and DBI, lower scores are better.

Model	Sil	WCSS	DBI
Our Model	0,58	36.279	0,60
Our Model (no loca)	$0,\!50$	175.329	0,65
PCA	0.53	447.094	$0,\!55$
CNN+Att	0.54	171.369	0,62
CNN+Mixer+Att	0.35	265.529	1,19

4 Conclusion

We have presented an architecture effectively captures complex patterns, and we also demonstrate that incorporating geographical information is crucial for learning high-quality representations. The embedding vectors work well in unsupervised clustering, proven effective on real data. Future work will explore applying these embeddings to downstream tasks such as forecasting and anomaly detection.

References

- 154 [1] I. Tolstikhin, N. Houlsby, A. Kolesnikov, L.
 155 Beyer, X. Zhai, T. Unterthiner, J. Yung, A.
 156 Steiner, D. Keysers, J. Uszkoreit, M. Lucic, and
 157 A. Dosovitskiy. MLP-Mixer: An all-MLP Ar158 chitecture for Vision. 2021. arXiv: 2105.01601
 159 [cs.CV]. URL: https://arxiv.org/abs/2105.
 160 01601.
- 161 [2] ADES. Portail national d'accès aux données
 162 sur les eaux souterraines. Consultation et ex163 portation des données: mesures de niveau d'eau,
 164 analyses de qualité, fiches descriptives des sta165 tions de mesure (piézomètres et qualitomètres).
 166 Eaufrance. URL: https://ades.eaufrance.
 167 fr/ (visited on 10/17/2025).
- [3] S. Wang, H. Wu, X. Shi, T. Hu, H. Luo, L.
 Ma, J. Y. Zhang, and J. Zhou. *TimeMixer: Decomposable Multiscale Mixing for Time Series Forecasting*. 2024. arXiv: 2405.14616 [cs.LG].
 URL: https://arxiv.org/abs/2405.14616.
- 173 [4] S. Wang, J. Li, X. Shi, Z. Ye, B. Mo, W. Lin, S.
 174 Ju, Z. Chu, and M. Jin. TimeMixer++: A Gen175 eral Time Series Pattern Machine for Universal
 176 Predictive Analysis. 2025. arXiv: 2410.16032
 177 [cs.LG]. URL: https://arxiv.org/abs/2410.
 178 16032.
- A. Krizhevsky, I. Sutskever, and G. E. Hin-[5]179 ton. "ImageNet Classification with Deep Con-180 volutional Neural Networks". In: Advances in Neural Information Processing Systems. Ed. 182 by F. Pereira, C. Burges, L. Bottou, and K. 183 Weinberger. Vol. 25. Curran Associates, Inc., 184 2012. URL: https://proceedings.neurips. 185 cc / paper _ files / paper / 2012 / file / 186 c399862d3b9d6b76c8436e924a68c45b-Paper. 187 pdf.
- 189 [6] O. Ronneberger, P. Fischer, and T. Brox. UNet: Convolutional Networks for Biomedical
 Image Segmentation. 2015. arXiv: 1505.04597
 192 [cs.CV]. URL: https://arxiv.org/abs/1505.
 193 04597.
- 194 [7] T. Chen, S. Kornblith, M. Norouzi, and G.
 195 Hinton. A Simple Framework for Contrastive
 196 Learning of Visual Representations. 2020. arXiv:
 197 2002.05709 [cs.LG]. URL: https://arxiv.
 198 org/abs/2002.05709.
- [8] B. Mougin, V. Bault, and J. Nicolas. "Du bul-199 letin de situation actuel au bulletin prévisionnel 200 : MétéEAU Nappes". In: Colloque "Gestion des 201 eaux souterraines". HAL Id: hal-02924734v1. V1 202 Submitted on 28 Aug 2020. Colloque "100 ans 203 d'hydrogéologie: SMEGREG (20 ans), AHSP 204 (30 ans) et ENSEGID (50 ans)". Talence, Bor-205 deaux, France, 2020. URL: https://brgm.hal. 206 science/hal-02924734v1. 207